The node-to-datum voltage vector V_i can then be found by using the relation

$$V_i = -\left[Y_{ni} + A_{ri}A_i^r\right]^{-1}\left[A_{ri}C_i + A_{ti}I_b^t\right]. \quad (30)$$

The solutions of φ on Γ_p allow the determination of the scattering parameter S_{ij} of the TE_{10} mode as follows:

$$S_{pp} = \int_0^{d_p} \varphi^{(p)}\left(x^{(p)} = 0, y^{(p)}\right) f_1^{(p)}\left(y^{(p)}\right) dy^{(p)} - 1 \quad (31)$$

$$S_{pq} = \left(\frac{\beta_1^{(p)}\hat{\epsilon}_{rq}}{\beta_1^{(q)}\hat{\epsilon}_{rp}}\right)^{1/2} \int_0^{d_p} \varphi\left(x^{(p)} = 0, y^{(p)}\right) f_1^{(p)}\left(y^{(p)}\right) dy^{(p)} \quad (32)$$

In (32), both $\hat{\epsilon}_{rp}$ and $\hat{\epsilon}_{rq}$ should be replaced by 1 for H-plane junctions.

V. Numerical Results

To demonstrate the validity and effectiveness of the method, computed results for various H- and E-plane waveguide discontinuities have been obtained and compared with other theories available. In the analysis, the first six evanescent higher order modes are used in (24).

Numerical results for two-port and multiport junctions are given in Figs. 3 and 4. The NMD method is applicable to the analysis of multimedia problems and can also be easily applied to the frequency range in which waveguide propagates multimodes. Fig. 5(a) shows an inhomogeneous junction and its discretization scheme. In this case the boundary conditions $\varphi_{\text{air}} = \varphi_{\text{dielectric}}$ and $\partial\varphi/\partial n|_{\text{air}} = -\partial\varphi/\partial n|_{\text{dielectric}}$ should be taken into account on the interface between air and dielectric. Fig. 5(b) shows the results of the magnitude of reflection coefficient obtained by the NMD method and the moment method [3], respectively, and good agreement is obtained. The NMD results of the transmission coefficients given by Fig. 5(c) are quite different from those of the moment method [3]. In the moment method, the transmission coefficients of the higher order modes are not zero at the cutoff values of ϵ_r. As a check on the accuracy of our solutions, the total power sums P_t^s have been evaluated and the power conservation condition is satisfied to an accuracy of $\pm 10^{-5}$. So the results given by the NMD method are convincing.

VI. Conclusion

In this paper a network model decomposition algorithm has been developed which permits the scattering matrices to be computed for arbitrarily shaped H- or E-plane junctions. Computed results for various H- and E-plane junctions are also given as a demonstration of the validity of the method. Our discussions and results obtained indicate that the network model decomposition method has the virtues of simplicity and generality, and so is a powerful tool for the analysis of waveguide discontinuity problems.

References

[1] Wen Geyi, "Numerical solution of transmission line problems by a network model decomposition method based on polygon discretization," *IEEE Trans. Microwave Theory Tech.*, vol. 38, pp. 1086–1091, Aug. 1990.

[2] N. Marcuvitz, *Waveguide Handbook*. New York: McGraw-Hill, 1951.

[3] Y. L. Chow and S. C. Wu, "A moment method with mixed basis functions for scattering by waveguide junctions," *IEEE Trans. Microwave Theory Tech.*, vol. MTT-21, pp 333–340, July 1973.

[4] M. Koshiba and M. Suzuki, "Applications of the boundary element method to waveguide discontinuities," *IEEE Trans. Microwave Theory Tech.*, vol. MTT-34, pp. 301–307, 1986.

Analysis of $E-H$ Plane Tee Junction Using a Variational Formulation

B. N. Das and N. V. S. Narasimha Sarma

***Abstract*—An analysis of an $E-H$ plane tee junction taking the width of the slot and wall thickness into account is presented. The parameters of the three-port equivalent network are determined. The reflection as well as transmission parameters are evaluated. A comparison between theoretical and experimental results is presented.**

I. Introduction

In the investigations on $E-H$ plane T junctions reported in the literature [1], the internal energy storage required for the evaluation of impedance loading has been found by regarding the coupling slot as a superposition of transverse and longitudinal components. Hsu and Chen [2] have presented a method of analysis which is not based on this concept. In the coordinate transformation they use, there is no scope for taking the effect of slot width into account. Further, in [2, eq. (8)] limits of integration were not properly taken. In the method suggested by Stevenson [3] and used by Elliott *et al.* [4] the expression involves a singularity, which, it is suggested, should be avoided for better accuracy. But the method for avoiding the singularity is not indicated.

In the present work, a three-port equivalent network for an $E-H$ plane tee junction is determined taking into account the effect of waveguide wall thickness and considering the contribution of the dominant mode to the imaginary part of the self-reaction.

From a knowledge of the equivalent network parameters, the net impedance loading, reflection coefficient, and coupling are evaluated for an $E-H$ plane tee junction. A comparison between theoretical and experimental results is also presented.

II. Analysis

The inclined slot-coupled $E-H$ plane tee junction together with the coordinate system is shown in Fig. 1. The three-port equivalent circuit of the junction is shown in Fig. 2. For a matched termination at port 3, the variational expression for the

Manuscript received September 26, 1990; revised April 3, 1991.

B. N. Das is with the Department of Electronics and Electrical Communication Engineering, Indian Institute of Technology, Kharagpur, 721 302 India.

N. V. S. Narasimha Sarma is with the Department of Electronics and Computer Science, Regional Engineering College, Warangal, 506 004 India.

IEEE Log Number 9102332.

0018-9480/91/1000-1770$01.00 ©1991 IEEE

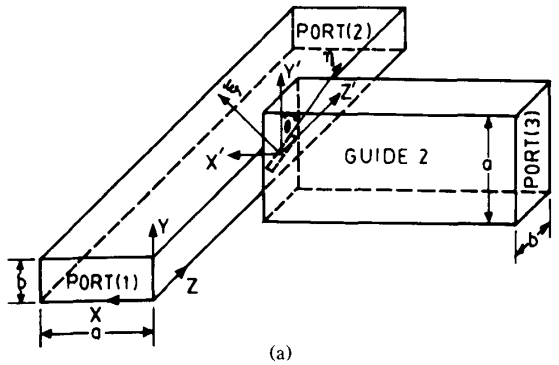

(a)

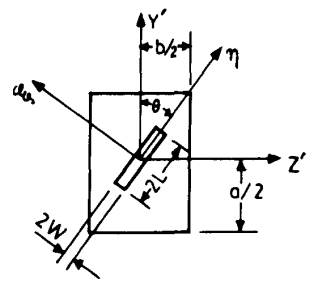

(b)

Fig. 1. Inclined slot-coupled coplanar $E-H$ plane tee junction.

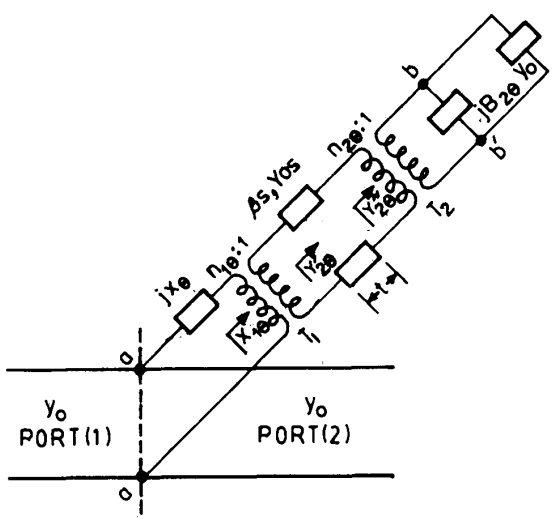

Fig. 2. Equivalent network representation.

admittance at plane $b-b'$ of Fig. 2 is of the form [5, eq. (2)]

$$Y_{2\theta} = Y_0 + jB_{2\theta} = \frac{\sum_m \sum_n \left[(V^e_{mn})^2 Y^e_{0mn} + (V^m_{mn})^2 Y^m_{0mn} \right]}{V^e_{10} V^e_{10}}. \quad (1)$$

Expressions for V^e_{mn}, V^m_{mn}, and V^e_{10}, in (1) are derived by following the procedure of [6, ch. 8] and using appropriate coordinate transformation for the structure of Fig. 1 assuming a slot field distribution of the form

$$\vec{E} = \vec{U}_\xi E_1 \cos \frac{\pi \eta}{2L}. \quad (2)$$

The turns ratio of the transformer (T_2) is of the form

$$\frac{1}{n_{2\theta}} = \frac{\sqrt{2LW}}{\sqrt{\frac{2}{ab}}\, 4W \frac{\sin\left(\frac{\pi W \cos\theta}{a}\right)}{\frac{\pi W \cos\theta}{a}} \frac{\pi}{2L} \frac{\cos\left(\frac{\pi L \cos\theta}{a}\right)}{\left(\frac{\pi}{2L}\right)^2 - \left(\frac{\pi \cos\theta}{a}\right)^2}}. \quad (3)$$

The admittance presented at the primary of the transformer (T_2) is expressed as

$$Y''_{2\theta} = (n_{2\theta})^{-2} Y_{2\theta}. \quad (4)$$

The expression for the admittance presented at the secondary of the transformer (T_1) owing to a transmission line of length t is of the form

$$Y'_{2\theta} = Y_{\varnothing s} \frac{Y''_{2\theta} + Y_{\varnothing s} \tanh \gamma_s t}{Y_{\varnothing s} + Y''_{2\theta} \tanh \gamma_s t} \quad (5)$$

where γ and $Y_{\varnothing s}$ are the propagation constant and characteristic admittance of the transmission line.

The turns ratio, $n_{1\theta}$, is obtained as

$$\frac{1}{n_{1\theta}} = \sqrt{\frac{\left(Y_0 \iint_s \hat{n} \times \vec{E} \cdot \vec{h}^{(1)}_{10}\, ds \right)^2}{V_{\text{Slot}} V_{\text{Slot}} Y'^2_{2\theta}}}. \quad (6)$$

In the above expression,

$$\vec{h}^{(1)}_{10} = \vec{U}_z \sqrt{2/ab} \cos(\pi z'/a) \quad (7)$$

and

$$V_{\text{slot}} = \sqrt{2LW}\, E_1. \quad (8)$$

From (2) and (6)–(8), the expression for n_{10} is obtained as

$$\frac{1}{n_{1\theta}} = \sqrt{\frac{Y^2 ab^3 \sin^2\theta \pi^2}{16LW (Y'_{2\theta})^2 \lambda_g^2} \left(\frac{\sin \beta W \cos\theta}{\beta W \cos\theta} \right)^{-2} \left[\frac{1 - (4L \sin\theta/\lambda)^2}{\cos(\beta L \,\text{sn}\,\theta)} \right]}. \quad (9)$$

The expression for the circuit parameter jX_θ is given by

$$jX_\theta = \frac{\iiiint_{\text{SLOT}} \hat{n} \times \vec{E}(\xi, \eta) \cdot j\bar{\bar{B}} \cdot \hat{n} \times \vec{E}(\xi', \eta')\, ds'\, ds}{Y_\theta^2 \left[\iint \hat{n} \times \vec{E} \cdot \vec{h}^{(1)}_{10}\, ds \right]^2}. \quad (10)$$

The spatial susceptance is of the form [2]

$$j\bar{\bar{B}} = (K^2 \bar{\bar{I}} + \nabla\nabla) \cdot \bar{\bar{G}} \quad (11)$$

where

$$\bar{\bar{I}} = U_x U_x + U_y U_y + U_z U_z \quad (12)$$

and

$$\bar{\bar{G}} = \sum_m \sum_n \frac{\epsilon_m \epsilon_n}{2ab\gamma mn} \exp[-\gamma_{mn}|z-z'|]X \cdot X\left[\vec{U}_x\vec{U}_x \sin\frac{m\pi x}{a}\sin\frac{m\pi x'}{a}\cos\frac{n\pi y}{b}\cos\frac{n\pi y'}{b} + \cos\frac{m\pi x}{a}\cos\frac{m\pi x'}{a}\left(\vec{U}_y\vec{U}_y \sin\frac{n\pi y}{b}\sin\frac{n\pi y'}{b} + \vec{U}_z\vec{U}_z \cos\frac{n\pi y}{b}\cos\frac{n\pi y'}{b}\right)\right] \quad (13)$$

Substituting (2), (7), and (9)–(13) and using appropriate coordinate transformation, the integration with respect to the variables ξ' and η' is first evaluated. The corresponding limits of the integration are taken from $-L$ to η, W to ξ, η to L, and ξ to $-W$. Before carrying out the integration, the dot product between dyadic and vector is evaluated using appropriate coordinate transformation for variables ξ and η and unit vectors $\vec{U}_\xi$ and $\vec{U}_\eta$. The variables ξ and η appearing in the expression are now replaced by y' and z' for the purpose of carrying out the differentiation appearing in the dyadic operator. After the differentiation the variables y' and z' are then transformed to ξ and η for the purpose of evaluating the double integral. The limits of the integration are now $-L$ to L for η and W to $-W$ for ξ. The final lengthy expression so obtained cannot be reproduced here for lack of space.

III. Estimation of Coupling, Reflection, and Transmission Coefficients

The coupling, reflection, and transmission coefficients seen from the primary guide are estimated. The normalized input impedance presented by the network at reference plane $a-a'$ is given by

$$Z_\theta = r_\theta + jx_\theta = \frac{jx_\theta}{Z_\theta} + n_{1\theta}^2 \frac{1}{Y_{\theta s}Z_\theta} \times \frac{Y_{\theta s} + Y''_{2\theta}\tanh\gamma_s t}{Y''_{2\theta} + Y_{\theta s}\tanh\gamma_s t}. \quad (14)$$

From the total impedance, the reflection coefficient is obtained as

$$\Gamma = -\frac{1}{2Z_\theta + 1} \quad (15)$$

$$\text{Return Loss (R.L.)} = 2\phi \log|\Gamma|. \quad (16)$$

The transmission coefficient from port (1) to port (2) is given by

$$T = 1 + \Gamma. \quad (17)$$

From power balance condition, the coupling coefficient is obtained as

$$C = 1 - |\Gamma|^2 - |T|^2 \quad (18)$$

$$\text{coupling in dB} = 10\log C. \quad (19)$$

IV. Numerical and Experimental Results

Using the expressions (1)–(19) the return loss and coupling are evaluated for $2L = 1.4$ cm, $2W = 0.08$ cm and $\theta = 45°$ over the frequency range 10.8–11.8 GHz for $t = 0$ as well as $t = 0.127$ cm. The results are presented in Figs. 3 and 4 respectively. The experimental results on return loss and coupling are also presented in the same figures for purposes of comparison.

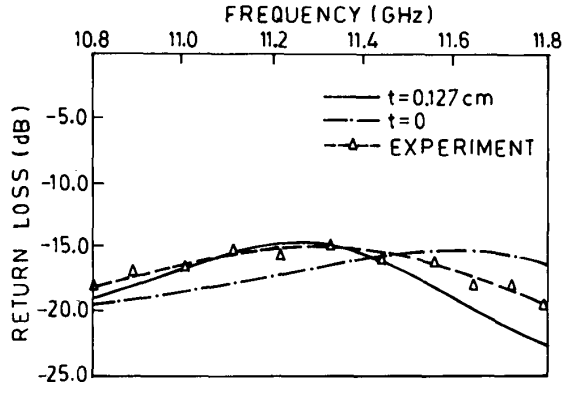

Fig. 3. Variation of return loss from port (1) with frequency for $2L = 1.4$ cm and $2W = 0.08$ cm.

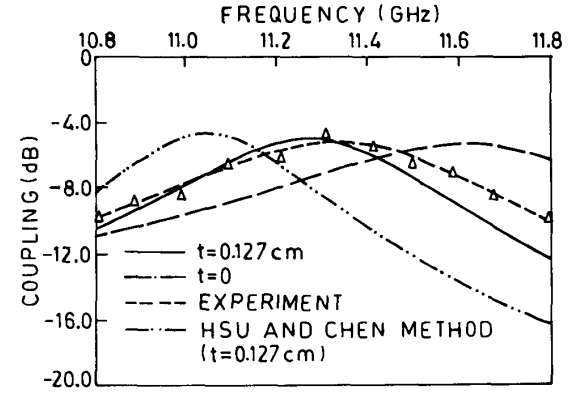

Fig. 4. Variation of coupling with frequency for $2L = 1.4$ cm and $2W = 0.08$ cm.

V. Discussion

The validity of the analysis presented in this work is established from the satisfactory agreement between the theoretical and experimental results. In this case the length of the coupling slot is around 1.4 cm, which corresponds to a free-space resonant frequency of 10.2 GHz. But the calculated resonant frequency is 11.2 GHz, which is higher than the free-space resonant frequency. It is worthwhile to state that for a slot of length less than $\lambda/2$, it has been observed by the authors that for a slot radiating into matched waveguide forming a tee junction, the length of the slot for resonance is greater than $\lambda/2$. The same is observed for a slot-coupled $E-H$ plane tee junction.

The deviation between the theoretical and experimental results is not appreciable for lower frequencies, but is found to increase at higher frequencies. This can be attributed to the fabrication irregularities of the coupling slot. As the frequency increases, the dimensional irregularities relative to wavelength increase, resulting in larger deviation between theoretical and experimental results with increasing frequency. Improvement in the bandwidth can be realized by using coupling slots with round ends.

References

[1] B. N. Das, G. S. N. Raju and A. Chakraborty, "Investigations on a new type of inclined slot coupled T-junction," *Proc. Inst. Elec. Eng.*, pt. H, vol. 134, pp. 473–476, 1987.

[2] Powen Hsu and S. H. Chen, "Admittance and resonant length of inclined slots in the narrow wall of a rectangular waveguide," *IEEE Trans. Antennas Propagat.*, vol. 37, pp. 45–49, Jan. 1989.

[3] A. F. Stevenson, "Theory of slots in rectangular waveguides," *J. Appl. Phys.*, vol. 19, pp. 24–38, Jan. 1948.

[4] R. S. Elliott *et al.*, "The scattering characteristics of broad wall slots," Hughes Technical Internal Correspondence, No. 56B1.31/111, Nov. 1, 1983.

[5] B. N. Das, N. V. S. Narasimha Sarma, and A. Chakraborty, "A rigorous variational formulation of an H plane slot coupled tee junction," *IEEE Trans Microwave Theory Tech.*, vol. 38, pp. 93–95, Jan. 1990.

[6] R. F. Harrington, *Time Harmonic Electromagnetic Field*. New York: McGraw-Hill, 1961.

[7] A. A. Oliner, "The impedance properties of narrow radiating slots in the broad face of rectangular waveguide—Parts I and II," *IEEE Trans. Antennas Propagat.*, vol. AP-5, pp. 4–20, Jan. 1957.

Theoretical and Experimental Study of the Evolution of Fields in an Overdimensioned Waveguide with a Corrugated Surface

J. P. Fenelon and A. Papiernik

Abstract—**The field of corrugated waveguides has been extensively investigated over a number of years, as such structures have been used for antenna feeds [1]–[4]. To obtain an answer to problems arising in many microwave applications, some labs use overdimensioned corrugated waveguides. In the present work, we propose a theoretical approach with eigenmodes that enables us to determine the values of the limiting frequencies (frequencies of π modes in the periodic structure) of an overdimensioned parallelepiped cavity loaded with a thin corrugation as a function of the height of the aperture. In this approach, the electric field is represented by different analytical functions. We compared the theoretical results with the experimental values obtained for different apertures and periodicities, according to the value of the wavelength in comparison with the aperture and the period. Each function is in good agreement in a certain frequency range.**

I. Introduction

In a previous study [5], we have shown experimentally that the dispersion characteristic of the periodic structure (period H) in Fig. 1 can be obtained with a cavity loaded by one corrugation (see Fig. 2). The length on either side of the zero-thickness corrugation is $L = kH$ (where k equal $1/2, 1, 3/2, \cdots$ according to the mode studied). The established mode always has the same configuration: the π mode (periodic phase shift $\beta H = \pi$ in the periodic structure).

We used the properties described above (for $L_1 = L_2 = H/2$, the resonant frequency of this cavity corresponding to the limiting frequency of the periodic structure with the same period H) and the "magnetic" eigenvectors to determine the expression for the magnetic field.

Manuscript received January 17, 1989; revised March 6, 1990.

J. P. Fenelon is with I.R.C.O.M., Facultédes Sciences, 123, Avenue Albert Thomas, 87060 Limoges Cedex, France.

A. Papiernik is with the Laboratorire d'Electronique, Université de Nice, Parc Valrose, 06034 Nice Cedex, France.

IEEE Log Number 9101653.

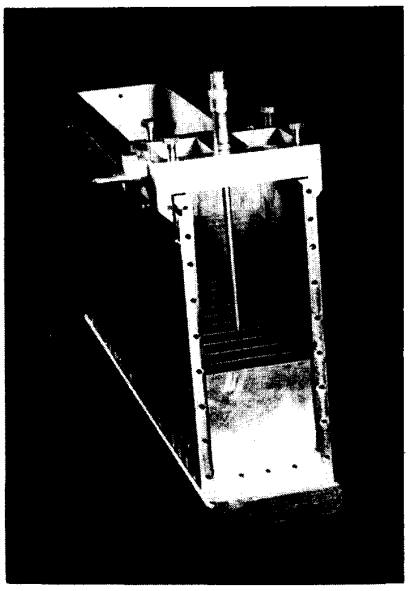

Fig. 1. An overdimensioned rectangular periodic waveguide.

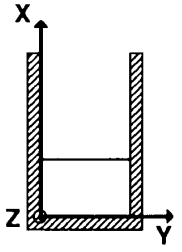

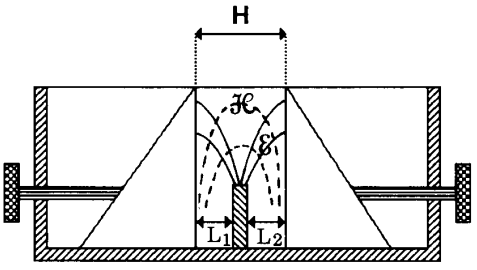

Fig. 2. Equivalent cavity with one corrugation to represent infinite periodic structure. Image of the field configuration in this cavity.

To obtain the theoretical resonant frequency, we assume that in the plane of the zero-thickness corrugation aperture ($x-y$ plane in Fig. 2) the expressions for the electric field components are $E_y = E_z = 0$ and $E_x = f(x)$, where for $f(x)$ we use a distribution, an exponential, and an inverse variation of the square of the distance from the aperture (see Fig. 3) and for the magnetic

0018-9480/91/1000-1773$01.00 ©1991 IEEE